Fluid Phase Equilibria 302 (2011) 161–168

Contents lists available at ScienceDirect

Fluid Phase Equilibria

journal homepage: www.elsevier.com/locate/fluid

On the prediction of ternary mixture phase behavior from the GC-SAFT-VR approach: 1-Pentanol + dibutyl ether + *n*-nonane

M. Carolina dos Ramos [a], Clare McCabe [a,b,*]

[a] Department of Chemical and Biomolecular Engineering, Vanderbilt University, Nashville, TN 37235, United States
[b] Department of Chemistry, Vanderbilt University, Nashville, TN 37235, United States

ARTICLE INFO

Article history:
Received 15 July 2010
Received in revised form 1 November 2010
Accepted 3 November 2010
Available online 16 November 2010

Keywords:
Equation of state
GC-SAFT-VR
Group contribution
Association
VLE
Ternary mixtures

ABSTRACT

In recent work [Peng et al. Fluid Phase Equilibr. 227(2) (2009), 131] a molecular-based group contribution SAFT-VR equation of state (GC-SAFT-VR) was proposed as a predictive tool for the study of fluid phase behavior. In the GC-SAFT-VR approach a fluid is modeled by a chain of tangentially bonded segments that each represent the different functional groups in the molecule, such as CH_3, CH_2 and OH, and so represents a more physically realistic model than that used in other SAFT-based approaches in which the segments of the model chain are identical i.e., have the same model parameters. The molecular parameters of the functional groups are determined by fitting to experimental vapor pressure and saturated liquid density data for selected members of different chemical families in a successive fashion, i.e., alkanes for CH_3 and CH_2 groups and subsequently alcohols for the OH group. The transferability of the molecular parameters can then be tested by comparing the theoretical predictions with experimental data for the phase behavior of pure fluids not included in the fitting process as well as binary mixtures of both *simple* fluids and polymer systems. Here, we continue the development of the GC-SAFT-VR approach, and for the first time, test its ability to predict the phase behavior of ternary mixtures. In particular, we consider binary and ternary mixtures of 1-pentanol, dibutyl ether and *n*-nonane. We find that the GC-SAFT-VR approach provides a good description of the phase equilibria of these binary and ternary systems without the need to fit cross interaction parameters to experimental mixture data.

1. Introduction

The statistical associating fluid theory (SAFT) is a molecular-based equation of state (EOS) developed by Chapman, Jackson and Gubbins [1–3], based on Wertheim's first-order perturbation theory (TPT1) [4–7], to study the thermodynamic behavior of complex fluids. In the SAFT approach, a fluid is described by a chain of tangentially bonded monomer segments that interact via dispersion, and association interactions if appropriate, with the free energy obtained from a sum of the different contributions that account for the monomer–monomer interaction, chain formation, and intermolecular association. Because the different microscopic effects are explicitly defined and accounted for, the SAFT approach has been shown to be a more predictive and reliable EOS than traditional cubic engineering equations. Since the introduction of the original SAFT expressions, many variations of SAFT have been proposed and the theory has been applied to study a wide range of fluid systems. For details the reader is directed to the comprehensive reviews of Müller and Gubbins [8], Economou [9], and more recently, McCabe and Galindo [10].

In recent years, there has been a focused effort to combine the SAFT equation with group contribution (GC) type approaches in order to expand the theory into a more powerful and predictive equation of state by reducing the amount of parameter fitting needed to study new systems. GC methods begin with the assumption that we can develop models for the interactions between molecules by decomposing these interactions into those between functional groups, and that such group-group interactions are transferable [11]. Hence, GC methods can be attractive techniques for estimating the phase equilibrium of complex fluids, as once parameters have been determined for a given functional group they should allow for accurate predictions of the phase behavior when combined with other groups.

Lora et al. [12,13] was the first to adopt and implement a GC method within SAFT to calculate the size and energy parameters of polyacrylates from group parameters determined from low-molecular-weight propanoates with the original homonuclear (i.e., all the segments in the model chain are identical) version of SAFT due to Huang and Radosz [14,15]. Subsequently, Tobaly and co-workers [16–22] introduced the GC-SAFT EOS, in which molecules

* Corresponding author at: Department of Chemical and Biomolecular Engineering, Vanderbilt University, Nashville, TN 37235, United States. Tel.: +1 865 974 0227; fax: +1 865 974 4910.
E-mail address: c.mccabe@vanderbilt.edu (C. McCabe).

0378-3812/$ – see front matter © 2010 Published by Elsevier B.V.
doi:10.1016/j.fluid.2010.11.003

are also described by a homonuclear model, but the parameters determined by averaging those for the functional groups within the molecule; the functional group parameters are in turn determined by fitting to experimental vapor pressure and saturated liquid density data for different chemical families in successive steps, according to the structure and composition of the molecule. In other related work Tihic et al. [23] have proposed a group-contribution PC-SAFT EOS that incorporates first and second order groups in an effort to describe proximity effects; however, the underlying chain model is homonuclear, and so all molecular heterogeneity is in fact lost. The next logical step in the development of a group-contribution approach within the SAFT framework is to implement a heteronuclear model to enable the differentiation of functional groups at the molecular level. This was done by Jackson et al. in the SAFT-γ [24,25] equation and by McCabe et al. in the GC-SAFT-VR [26–30] approach. Both approaches treat the monomer fluid as a mixture of different (i.e., heteronuclear) monomeric segments; the main difference between the two approaches lies in the treatment of the contribution to the free energy due to chain formation. While in the GC-SAFT-VR approach the heterogeneity of the segments is retained in the chain through a heteronuclear chain model, SAFT-γ uses effective parameters, determined from the segments in the monomer fluid, to describe a homonuclear chain. The functional group parameters in both approaches are determined in a similar manner by fitting the theory to experimental vapor pressure and saturated liquid density data for the smaller members of the chosen chemical families in successive steps. Once group parameters are obtained, the transferability of the parameters can then be tested by examining the phase behavior of larger molecular weight compounds that were not included in the parameter estimation process and through the study of mixture systems. The GC-SAFT-VR approach has been shown to accurately predict the phase behavior of both pure components and a number of binary mixtures in good agreement with experimental data and without fitting binary or cross interaction parameters to the mixtures being studied.

In an extension of previous work [28–30], to further probe the nature of the molecular interactions between different functional groups and examine the applicability of the theory to predict the phase behavior of ternary mixtures, we have studied the ternary system of 1-pentanol + dibutyl ether + *n*-nonane. This binary mixture was chosen primarily because it contains several different types of functional groups, both associating and non-associating. The inclusion of the associating (alcohol) and oxygenated (ether and alcohol) compounds can also lead to interesting phase behavior, including liquid–liquid immiscibility and azeotropy, that can be difficult to predict without experimental mixture data to fit cross interaction parameters to, and so this system provides a good test of the theory. In particular, we consider the prediction of the phase behavior of binary mixtures of 1-pentanol + dibutyl ether, 1-pentanol + *n*-nonane and dibutyl ether + *n*-nonane, as well as the phase behavior of the ternary mixture 1-pentanol + dibutyl ether + *n*-nonane at different thermodynamic conditions using the GC-SAFT-VR approach. The functional groups parameters needed to study these fluids i.e., CH_3, CH_2, OCH_2 ether, and a terminal OH functional group, were previously determined by fitting to experimental data for selected members of the relevant chemical families [28–30]; hence this is a purely predictive study.

2. Molecular model and theory

Within the GC-SAFT-VR approach [28–30] molecules are represented by a heteronuclear chain model that describes the different functional groups within each molecule being studied by unique segments. As with the SAFT-VR EOS [31,32], the dispersive interactions between segments that represent the functional groups are treated by a square-well (SW) potential. The interactions between a functional group of type *i* present in molecule *k* with a functional group of type *j* in molecule *l* is therefore represented by,

$$u_{ki,lj}(r) = \begin{cases} +\infty & \text{if} \quad r \le \sigma_{ki,lj} \\ -\varepsilon_{ki,lj} & \text{if} \quad \sigma_{ki,lj} \le r \le \lambda_{ki,lj}\sigma_{ki,lj} \\ 0 & \text{if} \quad r \ge \lambda_{ki,lj}\sigma_{ki,lj} \end{cases} \tag{1}$$

where $\sigma_{ki,lj}$, $\lambda_{ki,lj}$, and $\varepsilon_{ki,lj}$ are the diameter, the range and the well-depth of the SW interaction potential, respectively.

The GC-SAFT-VR equation is written within the SAFT framework in terms of the total Helmholtz free energy, expressed as a sum of four separate contributions corresponding to the ideal free energy (A^{ideal}), the segment-segment interactions (A^{mono}), the formation of bonds between segments (A^{chain}), and the association interactions (A^{assoc}). Hence, the free energy is written as,

$$\frac{A}{Nk_BT} = \frac{A^{ideal}}{Nk_BT} + \frac{A^{mono}}{Nk_BT} + \frac{A^{chain}}{Nk_BT} + \frac{A^{assoc}}{Nk_BT} \tag{2}$$

where N is the total number of molecules in the system, T is the temperature, and k_B is the Boltzmann constant. Since the theory has been previously presented [28–30], here we provide only a brief overview of the main expressions for each term as they pertain to ternary systems.

The ideal Helmholtz free energy of a mixture of *three* components is given by,

$$\frac{A^{ideal}}{Nk_BT} = \sum_{k=1}^{3} x_k \ln\, \rho_k \Lambda_k^3 - 1 \tag{3}$$

where $\rho_k = N_k/V$ is the molecular number density of component k, x_k is the mole fraction of component k, and Λ_k is the thermal de Broglie wavelength of component k.

The monomer free energy is given by a second-order high-temperature expansion using Barker and Henderson perturbation theory for mixtures [33–35],

$$\frac{A^{mono}}{Nk_BT} = \sum_{k=1}^{3}\sum_{i=1}^{n'_k} x_k m_{ki} a^M = \sum_{k=1}^{3}\sum_{i=1}^{n'_k} x_k m_{ki} \left(a^{HS} + \frac{a_1}{k_BT} + \frac{a_2}{(k_BT)^2} \right) \tag{4}$$

where the first sum is over the three components of the system and the second sum is over all n'_k types of functional groups (i.e., segments) within each component, and m_{ki} is the overall contribution to the chain length of the molecule from the functional group of type *i*, which is obtained from the number of functional groups of type *i* (ν_{ki}) and the chain length per functional group of type *i* (m_i) by $m_{ki} = \nu_{ki} m_i$. a^M is the free energy per monomer segment, which in turn is given as the sum of the free energy of the hard-sphere reference fluid (a^{HS}) plus the first (a_1) and second (a_2) perturbation terms associated with the attractive interactions $u_{ki,lj}(r)$ given by Eq. (1). As in previous works, the residual free energy of a multi-component hard-sphere reference system, a^{HS} is determined from the expression of Boublik [36] and Mansoori and co-workers [37]; the mean-attractive energy associated with the first perturbation term is treated in the context of the M1Xb mixing rule [32] and the second-order perturbation term is obtained using the local compressibility approximation [31].

The contribution to the free energy due to the formation of chains for a three component mixture of hetero-segmented SW monomer segments is given by,

$$\frac{A^{chain}}{Nk_BT} = -\sum_{k=1}^{3} x_k \sum_{ij} \ln\, y^{SW}_{ki,kj}(\sigma_{ki,kj}) \tag{5}$$

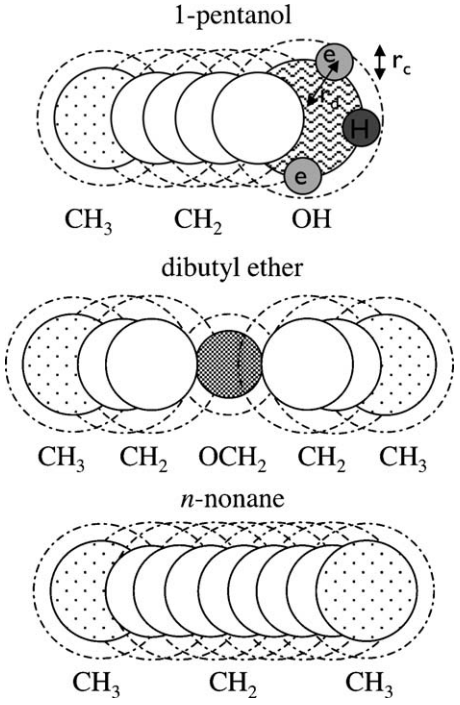

Fig. 1. Schematic representation of the molecular model used to describe 1-pentanol, dibutyl ether, and *n*-nonane molecules in the GC-SAFT-VR approach.

Table 1
Type and number of functional groups (ν_{ki}) used in the GC-SAFT-VR for the models of the 1-pentanol, dibutyl ether and *n*-nonane molecules.

Functional groups	1-Pentanol	Dibutyl ether	*n*-Nonane
CH_3 [28]	1	2	2
CH_2 [28]	4	5	7
OCH_2 ether [29]	0	1	0
OH terminal [30]	1	0	0

where the first sum is over all components in the mixture and the second sum considers the chain formation and connectivity of the segments within a given chain *k*. The background correlation function is in turn given by,

$$y^{SW}_{ki,kj}(\sigma_{ki,kj}) = \exp\left(\frac{-\varepsilon_{ki,kj}}{k_BT}\right) g^{SW}_{ki,kj}(\sigma_{ki,kj}) \tag{6}$$

where $g^{SW}_{ki,kj}(\sigma_{ki,kj})$ is the radial distribution function for the SW monomers at the contact distance $\sigma_{ki,kj}$ and is approximated by a first-order high-temperature perturbation expansion [31]. The exact form of Eq. (5) depends on the number of different types of segments and connectivity of the molecules being studied. The model for the ternary mixture of 1-pentanol (1) + dibutyl ether (2) + *n*-nonane (3) considered here is presented in Fig. 1 and the type and number of each functional group used to describe these molecules are reported in Table 1 and the number of bonds or connections between the different functional groups is presented in Table 2. Using this information, Eq. (5) is therefore given by,

Table 2
Type and number of bonds between the different functional groups used in the GC-SAFT-VR for the models of 1-pentanol, dibutyl ether and *n*-nonane molecules.

Connections or bonds	1-Pentanol	Dibutyl ether	*n*-Nonane
CH_3–CH_2	1	2	2
CH_2–CH_2	3	3	6
CH_2–OCH_2 ether	0	2	0
CH_2–OH terminal	1	0	0

$$\begin{aligned}\frac{A^{chain}}{NkT} = & -x_1\left[(m_{CH_3}-1)\ln y^{SW}_{1CH_3,1CH_3}(\sigma_{1CH_3,1CH_3}) + \ln y^{SW}_{1CH_3,1CH_2}(\sigma_{1CH_3,1CH_2})\right.\\ & +4(m_{CH_2}-1)\ln y^{SW}_{1CH_2,1CH_2}(\sigma_{1CH_2,1CH_2}) + 3\ln y^{SW}_{1CH_2,1CH_2}(\sigma_{1CH_2,1CH_2})\\ & \left.+(m_{OH}-1)\ln y^{SW}_{1OH,1OH}(\sigma_{1OH,1OH}) + \ln y^{SW}_{1CH_2,1OH}(\sigma_{1CH_2,1OH})\right]\\ & -x_2\left[2(m_{CH_3}-1)\ln y^{SW}_{2CH_3,2CH_3}(\sigma_{2CH_3,2CH_3}) + 2\ln y^{SW}_{2CH_3,2CH_2}(\sigma_{2CH_3,2CH_2})\right.\\ & +5(m_{CH_2}-1)\ln y^{SW}_{2CH_2,2CH_2}(\sigma_{2CH_2,2CH_2}) + 3\ln y^{SW}_{2CH_2,2CH_2}(\sigma_{2CH_2,2CH_2})\\ & \left.+(m_{OCH_2}-1)\ln y^{SW}_{2OCH_2,2OCH_2}(\sigma_{2OCH_2,2OCH_2}) + 2\ln y^{SW}_{2CH_2,2OCH_2}(\sigma_{2CH_2,2OCH_2})\right]\\ & -x_3\left[2(m_{CH_3}-1)\ln y^{SW}_{3CH_3,3CH_3}(\sigma_{3CH_3,3CH_3}) + 2\ln y^{SW}_{3CH_3,3CH_2}(\sigma_{3CH_3,3CH_2})\right.\\ & \left.+7(m_{CH_2}-1)\ln y^{SW}_{3CH_2,3CH_2}(\sigma_{3CH_2,3CH_2}) + 6\ln y^{SW}_{3CH_2,3CH_2}(\sigma_{3CH_2,3CH_2})\right]\end{aligned} \tag{7}$$

Finally, the contribution due to association interactions between sites on different functional groups that form the molecules being studied is expressed as,

$$\begin{aligned}\frac{A^{assoc}}{NkT} &= \sum_{k=1}^{3} x_k \sum_{i=1}^{n'_k} \nu_{ki} \sum_{a=1}^{ns'_i} n_{ia}\left(\ln X_{kia} + \frac{1-X_{kia}}{2}\right)\\ &= x_1 \sum_{i=1}^{n'_1} \nu_{1i} \sum_{a=1}^{ns'_i} n_{ia}\left(\ln X_{1ia} + \frac{1-X_{1ia}}{2}\right)\\ &= x_1 \cdot 1 \cdot \sum_{a=1}^{ns'_{OH}} n_{OHa}\left(\ln X_{1OHa} + \frac{1-X_{1OHa}}{2}\right)\end{aligned} \tag{8}$$

where the first sum is over the number of components *k*, the second sum corresponds to a sum over all types of functional groups in molecule *k* (n'_k), and the third sum over all sites on the functional group *i* (ns'_i). n_{ia} is the number of association sites of type *a* on each functional group of type *i*, and X_{kia} is the fraction of component *k* not bonded at site *a* on functional group *i*. Since there is only one functional group in the ternary mixture being studied that can form hydrogen bonds (i.e., the terminal OH functional group), and this functional group is only present in 1-pentanol molecule, the summations in the association contribution can be further simplified, as shown. As shown in Fig. 1, the hydrogen bonding association in the 1-alcohols is explicitly described in the GC-SAFT-VR approach by the inclusion of two types of associating sites on the terminal OH functional group [30]: one labeled type *H*, that represents the hydrogen atom, and two labeled type *e*, representing the lone pair of electrons in the oxygen atom, with only the *H*–*e* association interactions allowed, i.e., no *e*–*e* or *H*–*H* interactions are permitted. The non-bonded fractions X_{kia} are obtained from the solution of the mass-action equations [1–3] expressed in terms of the total number density of the system as,

$$X_{kia} = \frac{1}{1 + \rho \sum_{l=1}^{3} x_l \sum_{j=1}^{n'_l} \nu_{lj} \sum_{b=1}^{ns'_j} n_{jb} X_{ljb} \Delta_{kia,ljb}} \tag{9}$$

Here, $\Delta_{kia,ljb}$ depends on the strength of the association sites *a* and *b* located on groups *i* and *j* of components *k* and *l*, respectively, and is defined by,

$$\Delta_{kia,ljb} = K^{HB}_{kia,ljb} f_{kia,ljb} g^{SW}_{ki,lj}(\sigma_{ki,lj}) \tag{10}$$

where $K^{HB}_{kia,ljb}$, $f_{kia,ljb}$ and $g^{SW}_{ki,lj}(\sigma_{ki,lj})$ are the volume available for bonding, the Mayer *f*-function and the radial distribution function for the SW monomers, respectively. The Mayer *f*-function is given by $f_{kia,ljb} = \exp(-\varepsilon^{HB}_{kia,ljb}/k_BT) - 1$, where $\varepsilon^{HB}_{kia,ljb}$ is the well depth

Table 3
GC-SAFT-VR parameters for the chain length (m_i), segment size (σ_{ii}), segment–segment well-depth (ε_{ii}/k_B) and range (λ_{ii}), site–site association energy ($\varepsilon_{ii}^{HB}/k_B$) and bonding volume ($K_{ii}^{HB}$) of each functional group considered. The cross interaction parameters between functional groups are obtained through the Lorentz–Berthelot combining rules.

	CH_3	CH_2	OCH_2 ether	OH terminal
m_i	0.6670	0.3330	1.0000	0.1760
σ_{ii} (Å)	3.7370	4.0410	3.1235	5.2988
ε_{ii}/k_B (K)	234.250	237.230	180.266	534.805
λ_{ii}	1.492	1.667	1.690	1.495
$\varepsilon_{ii}^{HB}/k_B$ (K)	–	–	–	2797.000
K_{ii}^{HB} (Å^3)	–	–	–	0.1601

of the SW site–site interaction between sites a and b located on segments i and j of components k and l, respectively. The volume available for bonding is given by the expression:

$$K^{HB}_{kia,ljb} = \frac{4\pi\sigma^2_{ki,lj}}{72r_d^2}\left[\ln\left(\frac{r_{c_{kia,ljb}}+2r_d}{\sigma_{ki,lj}}\right)(6r^3_{c_{kia,ljb}}+18r^2_{c_{kia,ljb}}r_d-24r_d^3)\right.$$
$$+(r_{c_{kia,ljb}}+2r_d-\sigma_{ki,lj})(22r_d^2-5r_{c_{kia,ljb}}r_d-7r_d\sigma_{ki,lj}$$
$$\left.-8r^2_{c_{kia,ljb}}+r_{c_{kia,ljb}}\sigma_{ki,lj}+\sigma^2_{ki,lj})\right] \quad (11)$$

where r_d represents the distance from the center of the segment on which each site is located ($r_d/\sigma_{ki,lj}=0.25$), and $r_{c_{kia,ljb}}$ is the cut-off range between two sites a and b located on segments i and j of components k and l, respectively. For the ternary system being studied Eqs. (9)–(11) therefore become:

$$X_{1OHa} = \frac{1}{1+\rho x_1\cdot 1\cdot\sum_{b=1}^{ns'_{OH}} n_{OHb}X_{1OHb}\Delta_{1OHa,1OHb}} \quad (12)$$

$$\Delta_{1OHa,1OHb} = K^{HB}_{1OHa,1OHb}f_{1OHa,1OHb}g^{SW}_{1OH,1OH}(\sigma_{1OH,1OH}) \quad (13)$$

$$K^{HB}_{1OHa,1OHb} = \left[\frac{4\pi\sigma^2_{1OH,1OH}}{72r_d^2}\ln\left(\frac{r_{c_{1OHa,1OHb}}+2r_d}{\sigma_{1OH,1OH}}\right)(6r^3_{c_{1OHa,1OHb}}+18r^2_{c_{1OHa,1OHb}}r_d-24r_d^3)\right.$$
$$\left.+(r_{c_{1OHa,1OHb}}+2r_d-\sigma_{1OH,1OH})(22r_d^2-5r_{c_{1OHa,1OHb}}r_d-7r_d\sigma_{1OH,1OH}-8r^2_{c_{1OHa,1OHb}}+r_{c_{1OHa,1OHb}}\sigma_{1OH,1OH}+\sigma^2_{1OH,1OH})\right] \quad (14)$$

We note that unlike the original SAFT and SAFT-VR approaches in which association sites are not localized on a given segment within a chain but averaged over all segments, in the GC-SAFT-VR approach through the use of a hetero-segmented chain fluid we can now localize the association sites and their interactions on specific functional groups.

With the Helmholtz free energy defined, other thermodynamic properties, such as the chemical potential (μ_k) and pressure (P) can be easily obtained using standard thermodynamic relations.

3. Results

Our main interest in the current work is to demonstrate the versatility of the GC-SAFT-VR approach to predict the phase equilibria of associating ternary systems. For this purpose we have selected a representative ternary system, namely the mixture of 1-pentanol + dibutyl ether + n-nonane. The molecules of this mixture are composed of four different types of functional groups, i.e., the CH_3, CH_2, OCH_2 ether and terminal OH, the molecular parameters for which were obtained in previous work [28–30] by fitting to experimental vapor pressure and saturated liquid density data for selected members of the n-alkane, alkyl acetate, and linear alcohol chemical families using an annealing technique [38,39] in a step-wise procedure. These parameters are summarized in Table 3. The respective cross interactions between functional groups are obtained through the Lorentz–Berthelot combining rules for the unlike size and energy interactions by,

$$\sigma_{ki,lj} = \frac{\sigma_{ki,kj}+\sigma_{lj,lj}}{2} \quad (15)$$

$$\varepsilon_{ki,lj} = \sqrt{\varepsilon_{ki,ki}\varepsilon_{lj,lj}} \quad (16)$$

while the unlike potential range is given by,

$$\lambda_{ki,lj} = \frac{\lambda_{ki,ki}\sigma_{ki,ki}+\lambda_{lj,lj}\sigma_{lj,lj}}{\sigma_{ki,ki}+\sigma_{lj,lj}} \quad (17)$$

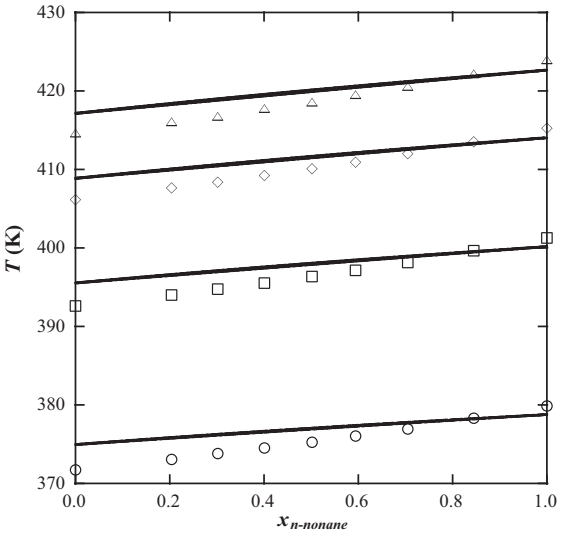

Fig. 2. Vapor–liquid equilibria for the binary mixture of dibutyl ether + n-nonane at 0.2666 bar (○), 0.5333 bar (□), 0.7999 bar (◊), and 1.0132 bar (△). Solid lines correspond to theoretical predictions from the GC-SAFT-VR approach and the symbols to experimental data [40].

Before studying the ternary system, we first consider the phase behavior of each of the binary mixtures formed from the components of the ternary mixture. For each binary mixture considered we have calculated the deviation of the theoretical predictions from experimental data as a percentage average absolute deviation in temperature (%AAD T) under isobaric calculations, as follows:

$$\%\text{AAD}\,T = \frac{1}{N_{pt}}\sum_{i=1}^{N_{pt}}\left|\frac{T_i^{\text{theo}}-T_i^{\text{exp}}}{T_i^{\text{exp}}}\right|\times 100\% \quad (18)$$

3.1. Dibutyl ether + n-nonane binary mixture

We first examine the binary mixture formed by dibutyl ether + n-nonane. As shown in Fig. 1, n-nonane is formed from two types of functional groups (CH_3 and CH_2), while dibutyl ether is composed of three types of functional groups (CH_3, CH_2 and OCH_2 ether). These two molecules have a similar number of carbon atoms and molecular weight and differ only in the presence of the OCH_2 functional group in dibutyl ether in place of two CH_2 groups in nonane. Fig. 2 presents the GC-SAFT-VR predictions for the vapor–liquid equilibria (VLE) of this mixture at different pressures. As can be seen from the figure, the theory predicts the

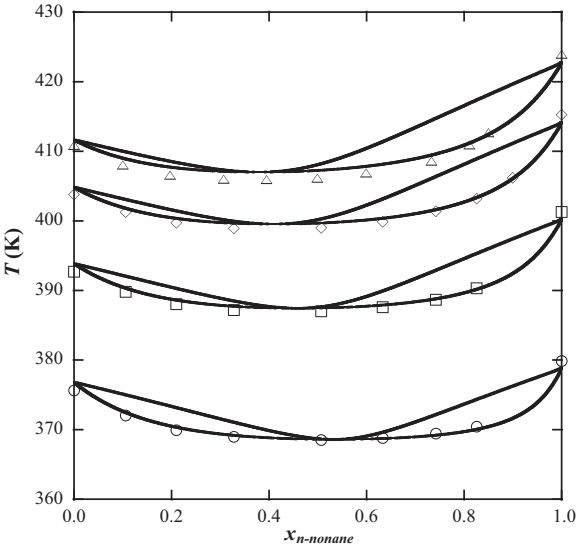

Fig. 3. Vapor–liquid equilibria for the binary mixture of 1-pentanol + *n*-nonane at 0.2666 bar (○), 0.5333 bar (□), 0.7999 bar (◊), and 1.0132 bar (△). Solid lines correspond to theoretical predictions from the GC-SAFT-VR approach and the symbols to experimental data [40].

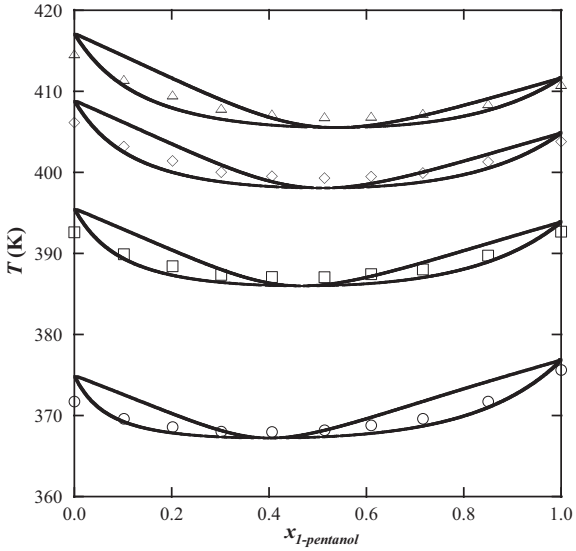

Fig. 4. Vapor–liquid equilibria for the binary mixture of 1-pentanol + dibutyl ether at 0.2666 bar (○), 0.5333 bar (□), 0.7999 bar (◊), and 1.0132 bar (△). Solid lines correspond to theoretical predictions from the GC-SAFT-VR approach and the symbols to experimental data [40].

VLE curves in good agreement with the experimental data. The similarity in molecular weight of the two components results in coexistence lines that are very close together, similar to the behavior seen when comparing the VLE of mixtures of isomers. Although there is a small over-prediction in temperature at compositions close to pure dibutyl ether, which could be due to the fact that relatively high deviations (11.02%) are seen in the GC-SAFT-VR predictions for the vapor pressure of dibutyl ether [29], we can see how describing the different functionality in the molecules enables a good description of the phase behavior, with average deviations in temperature of only 0.67%.

3.2. 1-Pentanol + n-nonane binary mixture

Constant pressure *Tx* slices of the 1-pentanol + *n*-nonane phase diagram at different pressures from 0.2666 bar to 1.0132 bar are presented in Fig. 3. This system is characterized by three functional groups representing the alcohol molecule (CH_3, CH_2, and OH linear) and two functional groups to represent the alkane molecule (CH_3 and CH_2), again with all parameters determined from pure component data without fitting to any experimental mixture data. As can be seen from the figure, the theoretical predictions from the GC-SAFT-VR approach are in excellent agreement with the experimental data, with average deviations in temperature of 0.37%. The theory is also able to accurately predict the presence of azeotropy, as well as the change in the azeotropic composition as the pressure is varied. If the chain length of the 1-pentanol or *n*-nonane is increased by the addition of CH_2 functional groups, the ability of the alcohol to self-associate should be hindered and hence, the azeotropic behavior disappear; although not shown this behavior is captured by the GC-SAFT-VR predictions.

3.3. 1-Pentanol + dibutyl ether binary mixture

We now consider the vapor–liquid equilibria for binary mixtures of pentanol and dibutyl ether. The theoretical predictions were again obtained using the parameters for the CH_3, CH_2, OCH_2 ether and the terminal OH functional groups determined in previous work [28–30]. In Fig. 4 we present the results for the binary mixture at different constant pressures and can see from the figure that the theory is able to predict the VLE curves in good agreement with the experimental data. Additionally the location of the minimum in temperature azeotrope is described accurately. The presence of the azeotrope in this mixture (Fig. 4), is again related to the ability of the alcohol molecule to self-associate; although not shown, as we increase either the 1-pentanol or dibutyl ether chain through the addition of more CH_2 functional groups, the azeotrope disappears as the self-association between the alcohol molecules is reduced. The excellent agreement between the theoretical predictions and experimental data obtained, with average deviations of %AAD $T = 0.33\%$, again demonstrates the capability of the GC-SAFT-VR approach to describe the fluid phase behavior of complex associating systems without fitting to the desired behavior.

3.4. 1-Pentanol + dibutyl ether + n-nonane ternary mixture

With the phase behavior of the binary mixtures characterized, we can apply the GC-SAFT-VR EOS to obtain the phase behavior of the ternary mixture at different thermodynamic conditions and test the transferability of the functional group parameters. The binary mixtures provide us with an accurate description of the phase behavior of the ternary system, since each axis of the ternary phase diagram is represented by the phase behavior of each binary mixture at the same temperature and pressure.

The liquid–vapor coexistence ternary diagrams for the mixture 1-pentanol + dibutyl ether + *n*-nonane at 0.2666 bar and several temperatures are presented in Fig. 5 and compared with the experimental data for the liquid phase by Kirss et al. [40]. In Fig. 5(a) the theoretical predictions of the coexistence boundaries for the system at 0.2666 bar and 368.09 K are presented. The phase behavior observed by the ternary system can be explained in terms of the phase behavior of the binary mixtures formed by the components of the ternary system. At 0.2666 bar, the binary system of 1-pentanol + dibutyl ether, as discussed earlier (see Fig. 4) exhibits azeotropic behavior, and so at the constant temperature of 368.09 K the vapor–liquid equilibria region in the ternary diagram can be found in two composition ranges: at low 1-pentanol compositions ($0.173 \leq x_1 \leq 0.305$) and at high 1-pentanol compositions ($0.508 \leq x_1 \leq 0.653$). At the same thermodynamic conditions, the binary systems 1-pentanol + *n*-nonane and dibutyl ether + *n*-nonane exhibit only one homogeneous liquid phase; it

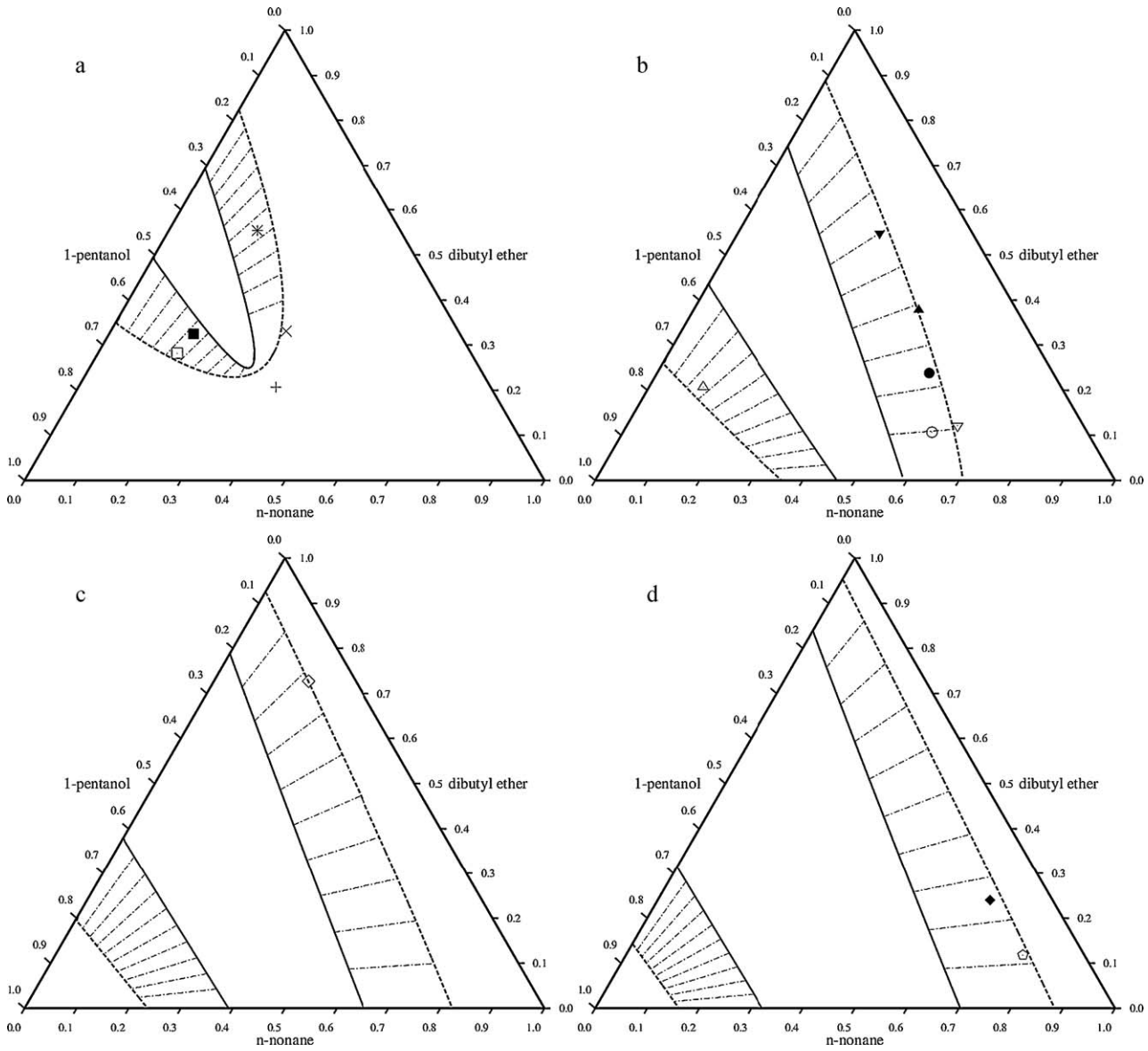

Fig. 5. Phase behavior for the ternary mixture 1-pentanol + dibutyl ether + *n*-nonane at 0.2666 bar and different temperatures: (a) 368.08 K, (b) 369 K, (c) 370 K, and (d) 371.17 K. The solid and dashed lines correspond to the theoretical predictions of the vapor and liquid coexistence boundaries from the GC-SAFT-VR approach, respectively; the dashed-dot lines represent the tie-lines between the phases in coexistence and the symbols correspond to experimental data [40] for boiling temperature isotherms (liquid phase) at values close to the four theoretical isotherms selected: 368.08 K (+), 368.19 K (×), 368.22 K (*), 368.32 K (⊡), 368.36 K (■), 368.75 K (○), 368.79 K (△), 369.14 K (●), 369.24 K (▲), 369.27 K (▽), 369.28 K (▼), 370.25 K (◊), 370.78 K (♦) and 371.17 K (⬠).

is therefore expected that the liquid–vapor coexistence curves in the ternary diagram at 0.2666 bar and 368.09 K will only meet the 1-pentanol + dibutyl ether axis and never reach the axes of other two binary mixtures. The liquid–vapor coexistence curves cross the 1-pentanol + dibutyl ether axis at four different points (two for each phase), corresponding to the four coexistence compositions of the binary mixture ($x_1^L = 0.173$ in coexistence with $x_1^V = 0.305$, and $x_1^L = 0.653$ in coexistence with $x_1^V = 0.508$). As we add *n*-nonane to the 1-pentanol + dibutyl ether mixture (i.e., increase the *n*-nonane composition), the liquid phase boundary moves from $x_1^L = 0.173$ to $x_1^L = 0.653$ and the vapor phase boundary moves from $x_1^V = 0.305$ to $x_1^V = 0.508$, without the lines crossing each other, and both passing through a maximum at 40–50% *n*-nonane. As we slightly increase the temperature to 369 K, as shown in Fig. 5(b), we can see how the two-phase (liquid–vapor) region increases in size and moves towards the 1-pentanol + *n*-nonane axis. At 0.2666 bar, the 1-pentanol + *n*-nonane binary mixture displays an azeotrope with a minimum in temperature at 368.60 K. This is represented in the ternary mixture diagram by a two-phase coexistence envelope that also crosses the 1-pentanol + *n*-nonane axis and divides the ternary diagram into 5 different regions: two liquid–vapor equilibria regions, two homogeneous liquid phase regions (one rich and one poor in 1-pentanol) and one homogeneous vapor phase region in the middle of the diagram. As the temperature is further increased to 370 K (Fig. 5(c)), the homogeneous liquid and vapor phases are clearly separated by two bands formed from the VLE regions that connect the 1-pentanol + dibutyl ether composition axis with the 1-pentanol + *n*-nonane composition axis. These bands move apart from each other as we increase the temperature to 371.17 K (Fig. 5(d)), resulting in a wider area where the homogeneous vapor phase can be found. A comparison with the available experimental data for the liquid phase boundary at similar thermodynamic conditions illustrates how the GC-SAFT-VR approach is able to accurately describe the phase behavior of the

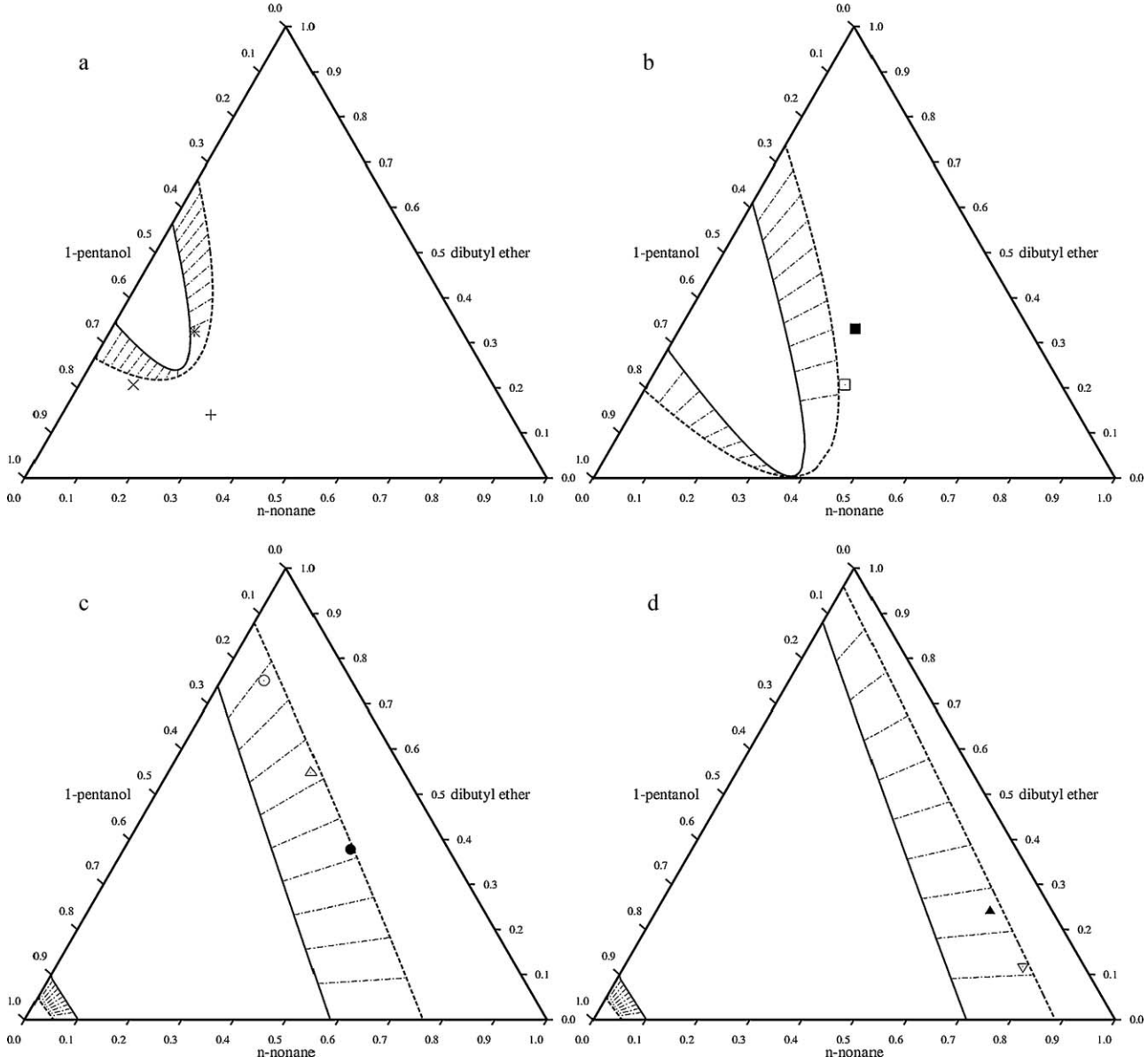

Fig. 6. Phase behavior for the ternary mixture 1-pentanol + dibutyl ether + *n*-nonane at 1.0132 bar and different temperatures: (a) 406.26 K, (b) 407 K, (c) 410 K, and (d) 413.86 K. The solid and dashed lines correspond to the theoretical predictions of the vapor and liquid coexistence boundaries from the GC-SAFT-VR approach, respectively; the dashed-dot lines represent the tie-lines between the phases in coexistence and the symbols correspond to experimental data [40] for boiling temperature isotherms (liquid phase) at values close to the four theoretical isotherms selected: 406.26 K (+), 406.84 K (×), 406.95 K (*), 407.05 K (⊡), 407.73 K (■), 410.13 K (○), 410.71 K (△), 410.75 K (●), 413.23 K (▲) and 413.86 K (▽).

1-pentanol + dibutyl ether + *n*-nonane mixture. We also note that the agreement can be considered to be very good given that the theory is capturing changes in the ternary diagram that occur over a small range of temperature values, i.e., from 368.09 to 371.17 K, which represents a ~3.08 K difference between part (a) and part (d) of Fig. 5.

We have also considered the effect of pressure by obtaining the phase behavior of the same ternary mixture at 1.0132 bar. As shown in Fig. 6, the ternary system exhibits similar behavior at 1.0132 bar as that seen at 0.2666 bar. At the lowest temperature studied (406.26 K), the liquid–vapor coexistence curves cross the 1-pentanol + dibutyl ether axis at four different points, corresponding to the four coexistence compositions for this binary mixture (Fig. 6(a)). As we increase the temperature to 407 K (Fig. 6(b)), the two-phase region crosses the 1-pentanol + *n*-nonane axis, dividing the ternary diagram into two liquid–vapor equilibria regions, two homogeneous liquid phase regions (one rich and one poor in 1-pentanol) and one homogeneous vapor phase region located between the two-phase areas. Once again, as we increase the temperature to 410 K (Fig. 6(c)), the one-phase regions are clearly separated by two two-phase bands connecting the 1-pentanol + dibutyl ether and 1-pentanol + *n*-nonane axes, which further separates as we go to 413.86 K (Fig. 6(d)). When comparing Fig. 5 with Fig. 6 we can see that although the general behavior is quite similar, the two-phase regions become smaller in size as the pressure is increased from 0.2666 to 1.032 bar. It is worth noting that, while the theory may not seem to provide as accurate a description of the system at the higher pressure (Fig. 6), it is not clear that this is the case. For example, comparing Figs. 5(a) and 6(a), it is possible that the theory over-predicts the effect of pressure on the system (in this case under-predicting the maximum in *n*-nonane composition at the higher pressure); however, it is not possible to make this assertion with confidence given the lack of experimental data (only 3 data points in the case of Fig. 6(a)). These results clearly

demonstrate the ability of the GC-SAFT-VR approach to accurately predict the phase behavior in complex ternary mixtures, without fitting the model parameters to any mixture data.

4. Conclusions

In this study we have tested the applicability of the GC-SAFT-VR approach to predict the phase behavior of the ternary system 1-pentanol + dibutyl ether + *n*-nonane. The GC-SAFT-VR approach is a molecular-based group contribution equation of state developed from the SAFT-VR equation that is able to accurately describe the effect of molecular functionality on fluid phase behavior through the explicit description of functional groups at both the monomer and chain levels of the theory. The functional group parameters for the molecules studied were obtained in previous work [28–30] by fitting to experimental vapor pressure and saturated liquid density data for selected members of the *n*-alkane, alkyl acetate and linear alcohol chemical families in a step-wise fashion. Using these parameters without modification, we have shown that the theory is able to accurately predict the phase behavior of binary mixtures of 1-pentanol + dibutyl ether, 1-pentanol + *n*-nonane and dibutyl ether + *n*-nonane, with average absolute deviations in temperature below 1%. We have also shown that the GC-SAFT-VR approach provides a very good description of the phase equilibria of the ternary system, given that the results are pure predictions and the model parameters are not fitted to experimental data for the binary or ternary systems being studied.

Acknowledgment

We gratefully acknowledge financial support from the National Science Foundation under grant number CBET-0829062.

References

[1] G. Jackson, W.G. Chapman, K.E. Gubbins, Phase equilibria of associating fluids spherical molecules with multiples bonding sites, Mol. Phys. 65 (1988) 1–31.
[2] W.G. Chapman, G. Jackson, K.E. Gubbins, Phase equilibria of associating fluids Chain molecules with multiples bonding sites, Mol. Phys. 65 (1988) 1057–1079.
[3] W.G. Chapman, K.E. Gubbins, G. Jackson, M. Radosz, New reference equation of state for associating liquids, Ind. Eng. Chem. Res. 29 (1990) 1709–1721.
[4] M.S. Wertheim, Fluids with highly directional attractive forces. 1. Statistical thermodynamics, J. Stat. Phys. 35 (1984) 19–34.
[5] M.S. Wertheim, Fluids with highly directional attractive forces. 2. Thermodynamic perturbation-theory and integral-equations, J. Stat. Phys. 35 (1984) 35–47.
[6] M.S. Wertheim, Fluids with highly directional attractive forces. 3. Multiple attraction sites, J. Stat. Phys. 42 (1986) 459–476.
[7] M.S. Wertheim, Fluids with highly directional attractive forces. 4. Equilibibrium polymerization, J. Stat. Phys. 42 (1986) 477–492.
[8] E.A. Müller, K.E. Gubbins, Molecular-based equations of state for associating fluids: a review of SAFT and related approaches, Ind. Eng. Chem. Res. 40 (2001) 2193–2211.
[9] I.G. Economou, Statistical associating fluid theory: a successful model for the calculation of thermodynamic and phase equilibrium properties of complex fluid mixtures, Ind. Eng. Chem. Res. 41 (2002) 953.
[10] C. McCabe, A. Galindo, SAFT Associating Fluids and Fluid Mixtures, Elsevier, Amsterdam, 2010.
[11] J.M. Prausnitz, R.N. Lichtenthaler, E.G. de Azevedo, Molecular Thermodynamics of Fluid-Phase Equilibria, 2nd ed., Prentice-Hall, New Jersey, 1986.
[12] M. Lora, M.A. McHugh, Phase behavior and modeling of the poly(methyl methacrylate)-CO_2-methyl methacrylate system, Fluid Phase Equilibr. 157 (1999) 285–297.
[13] M. Lora, F. Rindfleisch, M.A. McHugh, Influence of the alkyl tail on the solubility of poly(alkyl acrylates) in ethylene and CO_2 at High pressures: experiments and modeling, J. Appl. Polym. Sci. 73 (1999) 1979–1991.
[14] S.H. Huang, M. Radosz, Equation of state for small, large, polydisperse and associating molecules, Ind. Eng. Chem. Res. 29 (1990) 2284–2294.
[15] S.H. Huang, M. Radosz, Equaton of state for small, large, polydisperse and associating molecules: extension to fluid mixtures, Ind. Eng. Chem. Res. 30 (1991) 1994–2005.
[16] S. Tamouza, P. Passarello, P. Tobaly, J.C. de Hemptinne, Group contribution method with SAFT EOS applied to vapor liquid equilibria of various hydrocarbon series, Fluid Phase Equilibr. 222–223 (2004) 67–76.
[17] S. Tamouza, P. Passarello, P. Tobaly, J.C. de Hemptinne, Application to binary mixtures of a group contribution SAFT EOS (GC-SAFT), Fluid Phase Equilibr. 228–229 (2005) 409–419.
[18] T.X. Nguyen Thi, S. Tamouza, P. Tobaly, J.P. Passarello, J.C. de Hemptinne, Application of group contribution SAFT equation of state (GC-SAFT) to model phase behaviour of light and heavy esters, Fluid Phase Equilibr. 238 (2005) 254–261.
[19] T.X.N. Thi, S. Tamouza, P. Tobaly, J.-P. Passarello, J.-C. de Hemptinne, Application of group contribution SAFT equation of state (GC-SAFT) to model phase behaviour of light and heavy esters, Fluid Phase Equilibr. 238 (2005) 254–261.
[20] D. NguyenHuynh, A. Falaix, J.P. Passarello, P. Tobaly, J.C. de Hemptinne, Predicting VLE of heavy esters and their mixtures using GC-SAFT, Fluid Phase Equilibr. 264 (2008) 184–200.
[21] D. NguyenHuynh, J.P. Passarello, P. Tobaly, J.C. de Hemptinne, Application of GC-SAFT EOS to polar systems using a segment approach, Fluid Phase Equilibr. 264 (2008) 62–75.
[22] D. NguyenHuynh, M. Benamira, J.P. Passarello, P. Tobaly, J.C. de Hemptinne, Application of GC-SAFT EOS to polycyclic aromatic hydrocarbons, Fluid Phase Equilibr. 254 (2007) 60–66.
[23] A. Tihic, G.M. Kontogeorgis, N. von Solms, M.L. Michelsen, L. Constantinou, A predictive group-contribution simplified PC-SAFT equation of state: application to polymer systems, Ind. Eng. Chem. Res. 47 (2008) 5092–5101.
[24] A. Lymperiadis, C.S. Adjiman, A. Galindo, G. Jackson, A group contribution method for associating chain molecules based on the statistical associating fluid theory SAFT-gamma, J. Chem. Phys. 127 (2007) 234903.
[25] A. Lymperiadis, C.S. Adjiman, G. Jackson, A. Galindo, A. generalisation of the SAFT-gamma group contribution method for groups comprising multiple spherical segments, Fluid Phase Equilibr. 274 (2008) 85–104.
[26] C. McCabe, A. Gil-Villegas, G. Jackson, F. del Rio, The thermodynamics of heteronuclear molecules formed from bonded square-well (BSW) segments using the SAFT-VR approach, Mol. Phys. 97 (1999) 551–558.
[27] Y. Peng, H.G. Zhao, C. McCabe, On the thermodynamics of diblock chain fluids from simulation and heteronuclear statistical associating fluid theory for potentials of variable range, Mol. Phys. 104 (2006) 571–586.
[28] Y. Peng, K.D. Goff, M.C. dos Ramos, C. McCabe, Developing a predictive group-contribution-based SAFT-VR equation of state, Fluid Phase Equilibr. 277 (2009) 131–144.
[29] Y. Peng, K.D. Goff, M.C. dos Ramos, C. McCabe, Predicting the phase behavior of polymer systems with the GC-SAFT-VR approach, Ind. Eng. Chem. Res. 49 (2010) 1378–1394.
[30] M.C. dos Ramos, J.D. Haley, J.R. Westwood, C. McCabe, Associating functional groups in the GC-SAFT-VR approach: alcohols, aldehydes, amines and carboxylic acids, Fluid Phase Equilibr., submitted for publication.
[31] A. Gil Villegas, A. Galindo, P.J. Whitehead, S.J. Mills, G. Jackson, A.N. Burgess, Statistical associating fluid theory for chain molecules with attractive potentials of variable range, J. Chem. Phys. 106 (1997) 4168–4186.
[32] A. Galindo, L.A. Davies, A. Gil-Villegas, G. Jackson, The thermodynamics of mixtures and the corresponding mixing rules in the SAFT-VR approach for potencials of variable range, Mol. Phys. 93 (1998) 241–252.
[33] J.A. Barker, D.J. Henderson, Perturbation theory and equation of state for fluids – square-well potential, J. Chem. Phys. 47 (1967) 2856.
[34] J.A. Barker, D.J. Henderson, Perturbation theory and equation of state for fluids. 2. A successful theory of liquids, J. Chem. Phys. 47 (1967) 4714.
[35] J.A. Barker, D.J. Henderson, What is liquid – understanding states of matter, Rev. Mod. Phys. 48 (1976) 587–671.
[36] T. Boublik, Hard-sphere equation of state, J. Chem. Phys. 53 (1970) 471–472.
[37] G.A. Mansoori, N.F. Carnahan, K.E. Starling, T.W. Leland, Equilibrium thermodynamic properties of mixture of hard spheres, J. Chem. Phys. 54 (1971) 1523–1525.
[38] S. Kirkpatrick, C.D. Gelatt, M.P. Vecchi, Optimization by simulated annealing, Science 220 (1983) 671–680.
[39] W.B. Dolan, P.T. Cummings, M.D. Levan, Process optimization via simulated annealing – application to network design, AIChE J. 35 (1989) 725–736.
[40] H. Kirss, M. Kuus, E. Siimer, Isobaric vapor–liquid equilibria of the ternary system dibutyl ether + 1-pentanol plus nonane, J. Chem. Eng. Data 51 (2006) 1887–1891.